Dose effects on amorphous silicon sputtering by argon ions: A molecular dynamics simulation

Luis A. Marqués, José E. Rubio, Martn Jaraz, Luis A. Bailón, and Juan J. Barbolla

Citation: Journal of Applied Physics **81**, 1488 (1997); doi: 10.1063/1.363914
View online: http://dx.doi.org/10.1063/1.363914
View Table of Contents: http://scitation.aip.org/content/aip/journal/jap/81/3?ver=pdfcov
Published by the AIP Publishing

Dose effects on amorphous silicon sputtering by argon ions: A molecular dynamics simulation

Luis A. Marqués,[a] José E. Rubio, Martín Jaraíz, Luis A. Bailón, and Juan J. Barbolla
Departamento de Electricidad y Electrónica, Facultad de Ciencias, Universidad de Valladolid, 47011 Valladolid, Spain

(Received 22 July 1996; accepted for publication 28 October 1996)

We have investigated, using molecular dynamics techniques, the sputtering yield enhancement of amorphous silicon produced by argon ion accumulation within the target. Several amorphous silicon samples, with different argon contents, were bombarded with 1 keV argon ions at normal incidence. To study the influence of the target structure, we considered samples with different argon arrangements, either uniformly distributed or within solid bubbles. We have observed that silicon sputtering yield increases linearly with dose until steady state conditions are reached. This enhancement is produced by the shallow argon atoms through the weakening of Si–Si bonds. We have also observed that argon release takes place even long after the end of the collisional phase, and it is produced by ion-induced desorption and bubble destabilization. This enhanced argon yield determines the dose where target saturation and steady state conditions are reached. © *1997 American Institute of Physics.* [S0021-8979(97)06203-8]

I. INTRODUCTION

The sputtering of silicon produced by noble gas ions has been profusely studied both experimentally and theoretically due to its use in technological processes related to the microelectronic industry, such as etching, surface cleaning, profiling (secondary ion mass spectrometry), etc. Some experiments have been carried out to analyze the dependence of the sputtering yield on the ionic species,[1] on the ion energy,[2] and on the implanted dose,[2–5] as well as the angular distribution of the sputtered atoms.[6] All these experiments were carried out under high dose conditions, enough to amorphize the silicon samples. It was observed that the sputtering yield increased linearly with dose up to a steady state where it remained nearly constant.[2] It was also shown that steady state conditions were reached when the ion content of the sample saturated[2] and its surface was eroded to a depth close to the projected range of the ions.[4] Some authors have proposed different possible explanations to justify this behavior. For example, Blank and Wittmaack stated that the sputtering yield increase with dose is due to a ''wall effect'' produced by the ions incorporated near the target surface.[2] The accumulation of ions heavier than the target atoms generates a local increase of the target mass that favors the backscattering of subsequent ions and thus the deposition of the ion energy closer to the surface, consequently leads to an increase in the sputtering yield. On the other hand, Kirschner and Etzkorn justified the sputtering enhancement through the weakening of bonds among silicon atoms close to the target surface produced by the presence of the implanted ions.[4] Finally, Wittmaack proposed that this enhancement is due to displacements toward the surface of noble gas atoms previously implanted.[5] These atoms could drag silicon atoms in their way back to the target surface.

The silicon sputtering produced by noble gas ions has also been studied through the use of atomistic simulation techniques. In particular, the molecular dynamics method (MD) has been employed to get some insight on the silicon sputtering by low-energy argon ions.[7–9] The MD technique provides the individual trajectories of the atoms in a system by numerically solving the classical equations of motion.[10] These kinds of simulations were made possible after the development of empirical interatomic potentials making them capable of describing the covalent nature of silicon, such as the Stillinger–Weber[11] and Tersoff[12] potentials. Stansfield *et al.* used the Stillinger–Weber potential to study the dependence of the sputtering yield on the ion energy for several Ar–Si interaction potentials, and the angular and energy distributions of the sputtered atoms for the Si{100} and Si{100}(2×1) surfaces.[7] Smith *et al.* carried out the same kind of simulations using the Tersoff potential.[8] In both studies, yields and distributions were obtained by averaging the results of several hundreds of ion trajectories impinging on different target surface points. In each simulated trajectory, the ion enters a perfect crystal lattice at 0 K. Therefore, the simulation corresponds to a very low dose situation where target amorphization and ion accumulation do not occur. Surprisingly enough, the sputtering yields obtained in both studies for the Si{100} surface were very close to that experimentally measured by Zalm for a very high dose (well over the silicon amorphization threshold) and steady state conditions (target saturated with argon atoms).[1]

In a previous article, we studied the influence of target amorphization on the sputtering of silicon produced by 1 keV argon ions carrying out MD simulations using an amorphous target.[9] Our results indicated that the sputtering yield for an amorphous sample is lower than for Si{100} and Si{100}(2×1) crystal samples. This peculiar result is due to the fact that the surface atoms in the amorphous sample are more strongly bound to the substrate than in the case of crystal samples, since their average coordination is higher. Therefore, the cause responsible for the yield increase with dose must be related not to the target amorphization but to the accumulation of ions within the target. In this article, we

[a]Electronic mail: lmarques@alpha2.ele.cie.uva.es

 0021-8979/97/81(3)/1488/7/$10.00

present MD simulations carried out to determine the influence of the implanted argon on the sputtering process. In Sec. II, we describe the interatomic potential set used, the procedures followed to generate the samples, and the conditions of the bombardment simulations. In Sec. III, we present and discuss our results, and in Sec. IV the main conclusions of this work.

II. MOLECULAR DYNAMICS SIMULATIONS

A. Interatomic potential set

We have used the Stillinger–Weber potential[11] to describe the interactions among silicon atoms. This potential provides a good overall description of ion-induced damage in silicon.[13] Since the two-body term of the Stillinger–Weber potential does not represent accurately enough the high energy interactions, we splined it to the universal potential[14] at short distances. We also used the universal potential to describe the interactions between the argon ion and the target silicon atoms, with a cutoff radius of 4.8 Å. To reproduce the Ar–Ar interactions, we have used the Lennard–Jones potential with the typical parametrization for argon (σ=3.405 Å and ϵ=0.01 eV),[10] which has been shown to describe fairly well both liquid and solid phases of argon. The cutoff radius used for the Lennard–Jones potential was $r_c=2.5\ \sigma$. Both cutoff radii were chosen large enough to not introduce significant drifts in the total energy of the simulated system. To our knowledge, an empirical interatomic potential describing accurately the Ar–Si interaction for low energies has not been developed. However, since there is some experimental evidence that this interaction is purely repulsive in nature,[15] we also used the universal potential to describe the interaction between silicon and the argon atoms that are within the target, even though they only have vibrational energy. As we shall see, with this relatively simple set of interatomic potentials it is possible to reproduce, at least qualitatively, all of the experimental observations.

B. Sample preparation

A full MD simulation accounting for the dynamical accumulation of ions inside the target would be very time consuming, since it would require a very large sample and times between successive ions long enough to achieve thermal stabilization. Therefore, we followed an alternative procedure to study the sputtering process. This consists of preparing several silicon samples with different argon contents. Each of these samples represents a different stage in the sputtering experiments. First, we created a pure amorphous silicon sample at 300 K by melting and subsequently quenching a perfect 8000-atom crystal lattice, whose dimensions were $76.8\times76.8\times27.2$ Å^3, using periodic boundary conditions. The cooling rate was $\sim6.3\times10^{13}$ K s^{-1}, slow enough to get an amorphous structure instead of a supercooled liquid. The details of the amorphous sample preparation are given elsewhere.[9] In an identical volume to the previously mentioned for the amorphous silicon sample, we prepared several argon gases of different densities at 300 K, also using periodic boundary conditions. Each of the argon gases were mixed with the amorphous silicon sample, just by overlapping both samples in the same MD simulation cell (see Fig. 1). Using this procedure, some of the argon atoms may lie very close to silicon atoms, thus giving rise to very strong repulsive interactions. These interactions have to be relaxed before starting the bombardment simulations, since they may lead to target destabilization (vaporization). For this reason, it is necessary to allow the atoms to relax and, at the same time, to drain the kinetic energy released during the process. This can be done through frequent re-scaling of the atom velocities at 0 K (every 3 fs for 10 ps). Once the samples were well relaxed, some of them (B1 and B2 in Table I) were melted and afterwards quenched using the same cooling rate as in the case of the pure amorphous sample, down to a temperature of 300 K. During the cooling process, the argon atoms rearranged themselves leading to the formation of bubbles. Once the samples were stabilized, the periodic boundary conditions along the Z direction (the direction of incidence of the argon ions in the bombardment simulations) were removed and the sample was allowed to relax for another 40 ps. Since the samples had two free surfaces, this

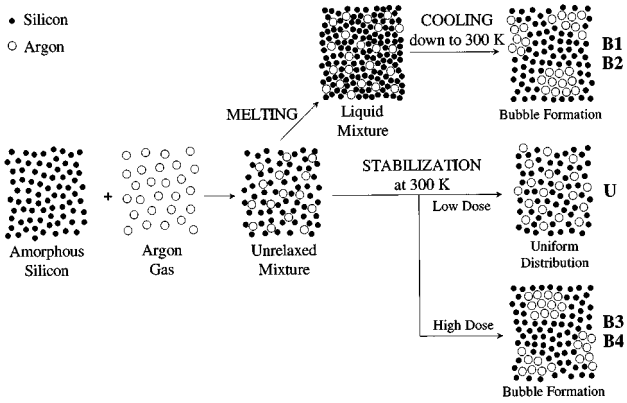

FIG. 1. Schematic representation of the generation procedures of the argon implanted silicon samples. The complete description is given in the text.

TABLE I. Characteristics of the amorphous silicon samples with different argon contents.

Sample	No. of argon atoms and at. %	heated to melting point	arrangement of argon atoms	maximum bubble radius (Å)
U	870 (9.8%)	NO	Uniform	···
B1	259 (3.1%)	YES	Bubbles	8
B2	1100 (12.1%)	YES	Bubbles	20
B3	1664 (17.2%)	NO	Bubbles	14
B4	2289 (22.2%)	NO	Bubbles	16

relaxation was at constant pressure conditions and thus they could change their volume to accommodate their different argon contents. We also prepared several samples (U, B3, and B4 in Table I) without heating them above room temperature in order to avoid bubble formation. The sample preparation procedures are sketched in Fig. 1. In both sample preparation schemes, during the final stabilization process at 300 K, some of the argon atoms located close to the free surfaces of the samples were desorbed, due to the purely repulsive nature of the Ar–Si interaction. As a consequence, no argon atoms remained in the regions within 5 Å from each free surface. This desorption process of the shallow argon atoms has also been experimentally observed.[15]

The characteristics of all the samples are shown in Table I. In sample U, most argon atoms became uniformly distributed. On the other hand, in samples B3 and B4 they rearranged themselves into bubbles, even though both samples were kept at room temperature. This result is in agreement with some experiments where it has been observed that for low doses the incorporated argon atoms become uniformly distributed, and for high doses they form bubbles due to the low solubility of argon in silicon.[15–20] These bubbles have proven to be very stable, to the point of being present within the target even after postbombardment annealing processes.[16,17] In our simulations, the bubble formation takes place when the argon concentration is so high (above 15%) that the argon atoms are closer in average than the cutoff distance of the Ar–Ar potential. Under these conditions, the argon atoms attract each other and form bubbles, even if the temperature (and thus the atom mobility) is kept low.

As can be seen in Table I, the sizes of the bubbles in samples B3 and B4 are smaller than in the case of sample B2, although the argon concentration is higher, due to the fact that the temperature during the generation of the first two samples was kept low and the argon atoms did not have enough time to form large bubbles. It has been observed experimentally that the argon bubbles are solid and overpressurized by the surrounding silicon.[20] This behavior is also observed in our samples, as it can be deduced by inspection of Fig. 2, where the pair distribution function $g(r)$ for the argon atoms in sample B4 is shown. The sharp first peak together with the broad feature around 6 Å is indicative of an amorphous structure. It is under compressive stress, since the distance of the first peak (3.25 Å) is 5% lower than the corresponding to the Ar–Ar potential minimum. The pair distribution functions of the bubbles in samples B1, B2, and B3 are very similar to that of Fig. 2.

C. Ion bombardment simulations

All of the samples displayed in Table I were bombarded with 1 keV argon ions at normal incidence along the Z direction (perpendicular to one of the free surfaces). Periodic boundary conditions were applied along the X and Y directions. When considering perfect crystal targets it is possible to define an *irreducible symmetry zone* reproducing all of the possible bombardment impact points.[21] However, when dealing with amorphous targets this zone can not be defined since there is no periodicity. In that case, to achieve good statistics, it is necessary to use samples with relatively large

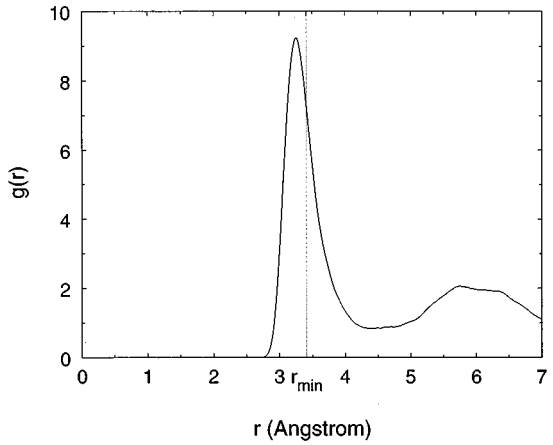

FIG. 2. Pair distribution function of the argon bubbles in sample B4, exhibiting the typical features of an amorphous structure. As it can be observed, the first peak is at a distance shorter than the corresponding to the potential minimum, $r_{\min}$, which means that the bubbles are under compressive stress produced by the surrounding silicon atoms.

surfaces and to simulate some thousands of ion trajectories entering through points randomly chosen across the whole surface. Besides, the target must be thick enough to encompass the whole sputtering process for a given ion energy. These conditions are fulfilled with the size of the samples described above, as it was demonstrated in a previous article.[9]

The equations of motion for each atom were integrated in time using a fourth order Gear predictor-corrector algorithm.[22] We employed a time-saving scheme which provides an important reduction in the computational time required for the calculation, based on the selective integration of the particles according to their respective energies.[23] Since the sputtering process takes place during the first stages of the collision cascade, it is enough to simulate each ion trajectory for just 500 fs.[8] Once the simulation of one ion is finished, we start the next ion using the same initial undamaged sample. Consequently, we are simulating low dose rate bombardment conditions, with no damage build up. Along the simulation of each ion cascade, the data associated to the sputtered atoms and backscattered ions (velocity, time, energy, etc.) are recorded. After the simulation of several thousands of ion cascades, those data are used to get statistical averages.

III. RESULTS AND DISCUSSION

The results of our simulations are summarized in Table II, where the total number of simulated ion trajectories and the sputtering yields for silicon and argon are given. For the sake of completeness, we also include the results obtained in a previous work on the bombardment of a pure amorphous silicon sample.[9] As it can be observed, sputtering yields increase with increasing argon concentration in the target. However, though sample U has an argon content smaller than sample B2, the corresponding silicon and argon yields are 1.1 and 2.3 times higher, respectively. We will try to justify these results afterwards.

TABLE II. Total number of simulated ion trajectories and sputtering yields obtained for each of the samples described in Table I. Results from the bombardment of a pure amorphous silicon (*a*-Si) are also included.

Sample	(% Ar)	Simulated ions	Silicon yield Y_{Si}	Argon yield Y_{Ar}
a-Si	(0%)	2909	0.39±0.02	···
U	(9.8%)	2181	0.54±0.03	0.18±0.03
B1	(3.1%)	3964	0.43±0.01	0.03±0.01
B2	(12.1%)	2824	0.49±0.02	0.08±0.02
B3	(17.2%)	2118	0.61±0.03	0.19±0.03
B4	(22.2%)	1987	0.68±0.03	0.25±0.03

In order to investigate the cause of the silicon sputtering enhancement, we studied the contributions to the yield from ions producing the sputtering of one to eight atoms, which are displayed in Fig. 3. In the case of samples with bubbles, the contribution from ion events leading to the ejection of more than one atom increases with increasing argon content. These contributions are 50% for *a*-Si, 54% for B1, 59% for B2, 70% for B3, and 76% for B4. Surprisingly, argon content does not seem to affect the contributions to the yield of events producing the sputtering of one silicon atom, which are similar for all samples within statistical error. Consequently, the enhancement of the silicon sputtering yield is due to the relative increase of the number of ion trajectories leading to the ejection of more than one atom. These trajectories are, in turn, closely related to the position of shallow argon atoms, as shown in Fig. 4 for the case of sample B4 (the results for the rest of the samples are very similar).

Therefore, it is clear that the argon atoms which are close to the target surface are the responsible for the yield enhancement. As it was already mentioned in Sec. I, several authors have proposed different mechanisms to justify this enhancement. Blank and Wittmaak suggested that it is produced by a wall effect created by the heavier shallow argon atoms.[2] To validate this hypothesis, we carried out MD simulations assuming the mass of the argon atoms in sample B4 to be equal to the silicon mass while maintaining the same interaction potentials. In this way, it is possible to study the

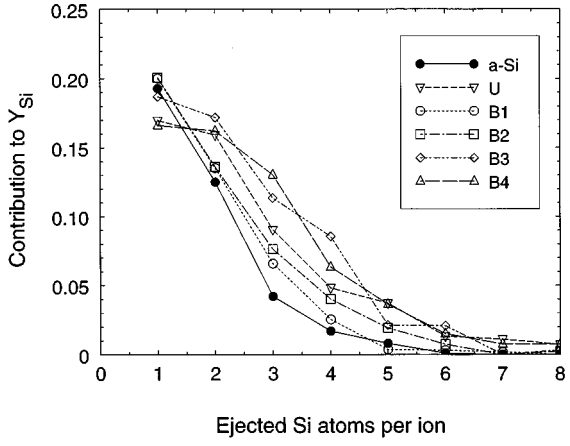

FIG. 3. Contribution to the silicon sputtering yield as a function of the number of ejected atoms. The addition of all the contributions give the sputtering yield Y_{Si} for each sample.

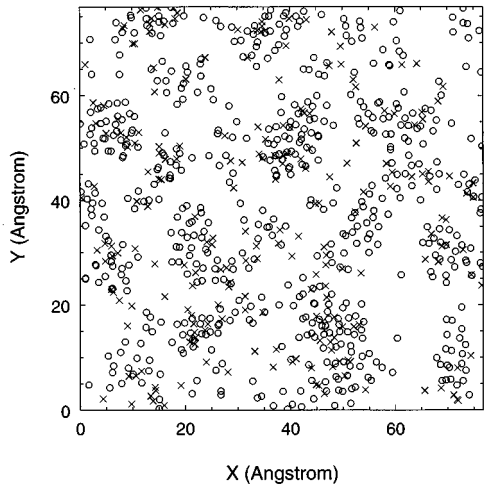

FIG. 4. Front view of sample B4. Circles represent the position of the shallower argon atoms (closer than 15 Å to the surface) and crosses the points of incidence of ions that produced the ejection of more than one atom. There is a clear correlation between crosses and circles, showing that the relative increase in the number of high-yield ion trajectories is due to the presence of argon atoms close to the target surface.

influence of the implanted species mass on the sputtering process. This new sample, that will be referred to as C, was bombarded under the same conditions that the ones previously mentioned: 1 keV argon ions at normal incidence. The results obtained are shown in Table III, along with those corresponding to B4. Even though the mass of the implanted species has been reduced by 30%, the total yield has decreased only by 6%. Besides, there is no appreciable change in the percentages of trajectories that produce the ejection of one, two, or more than two atoms. This result shows that the sputtering preferentiability must be related to the binding energies of the different elements, and not to their respective masses.

On the other hand, Wittmaak proposed that yield enhancement is produced because argon atoms sputtered from the sample drag silicon atoms on their way to the surface.[5] The results of our simulations do not favor this explanation. The time-of-escape distributions for sputtered atoms in sample B4 are represented in Fig. 5 (the distributions for the rest of the samples are very similar). Clearly, there is no correlation between the time of escape of silicon atoms and those corresponding to argon atoms. While silicon ejection ends around $t=300$ fs (as in the pure amorphous silicon sample bombardment), the escape of argon atoms continues beyond 500 fs. The ejection of argon atoms takes place mainly when an incoming ion impinges on a surface point

TABLE III. Sputtering yields obtained in the bombardment of sample C (see the text). For the sake of comparison, we also show the results from sample B4.

Sample	Simulated ions	Silicon yield Y_{Si}	Argon yield Y_{Ar}
B4	1987	0.68±0.03	0.25±0.03
C	2466	0.62±0.02	0.25±0.02

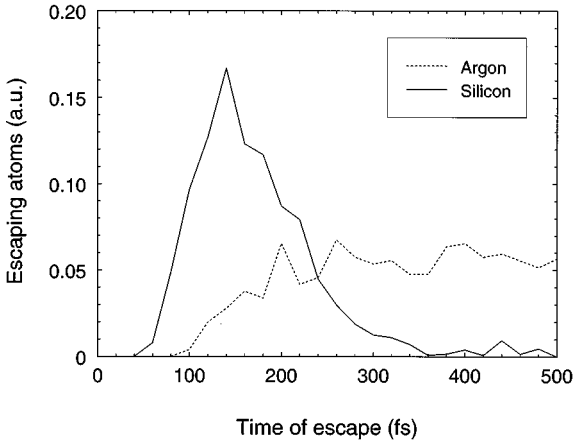

FIG. 5. Time-of-escape distributions for silicon and argon atoms obtained in the bombardment of sample B4. The much shorter ejection time of the silicon atoms rules out the possibility of them being dragged by escaping argon atoms.

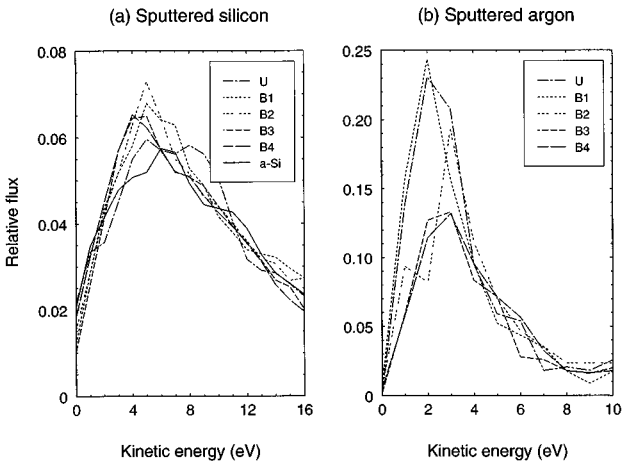

FIG. 6. Kinetic energy distributions of the sputtered (a) silicon atoms, and (b) argon atoms, obtained during the bombardment of the samples displayed in Table I. Results from the bombardment of a pure amorphous silicon sample are also included. The histogram bin size is 1 eV.

close to a shallow bubble. Usually, the impact produces the sputtering of some of the surface silicon atoms that cover the bubble, leading to the emission of some argon atoms, even after the end of the collisional phase of the cascade. In fact, for Ar atoms ejected after 300 fs, it seems more appropriate to think of bubble evaporation rather than of a true sputtering (collisional) process. The argon ejection is also favored by the pressure existing within the bubbles. In our simulations, all those argon atoms that escaped for times above 300 fs were ejected with kinetic energies lower than 5 eV, which is not enough to produce the sputtering of silicon atoms. However, there is probably sputtering of silicon atoms by this process when the pressure inside the bubbles (and, consequently, the kinetic energy of the released argon atoms) is higher, as it has been observed in some experiments.[20]

Considering our results, the more likely explanation to justify the sputtering yield enhancement is the one given by Kirschner and Etzkorn: the implanted argon atoms weaken the Si–Si bonds.[4] This can be also inferred from inspection of Fig. 6, where the energy distributions of the sputtered silicon and argon atoms are represented. As before, we include results from a pure amorphous silicon sample.[9] It has been pointed out by several authors that the position of the maximum in these distributions is directly related to the surface binding energy of the corresponding element in the target.[24–26] As it can be seen from Fig. 6(a), the maximum of the distribution for the pure amorphous silicon sample is located at an energy (6 eV) higher than for the other samples. This agrees with the fact that argon atoms weaken the Si–Si bonds. The lowest peak energy corresponds to sample B4 (4 eV) where there are a relatively high number of argon bubbles very close to the target surface. In the case of the energy distributions of the sputtered argon, the maxima are for lower energies, between 2 and 3 eV, in correspondence with Ar–Ar bonds being weaker than Si–Si bonds. For samples U and B1, where argon atoms are uniformly distributed and the bubbles are relatively small, respectively, the maxima are for an energy of 2 eV, while in the case of samples B2, B3, and B4 the maxima are for a higher energy, 3 eV. This result could have been anticipated, since the only source for an attractive interaction in the case of argon atoms is in the Ar–Ar interatomic potential. Besides, we have observed that the maxima in Fig. 6(b) are related to argon atoms released after the collisional phase of the cascade. This behavior is in agreement with some experiments[18,27] which show that the energy distributions of the argon atoms ejected during the bombardment of argon-preimplanted silicon samples exhibits two maxima: one at low energies associated to isolated atoms and another at higher energies, related to atoms in bubbles.

There are two main reasons behind this Si–Si bond weakening: first, the potential well is less deep for those silicon atoms that are close to argon atoms since the Ar–Si interaction is purely repulsive, and second, argon atoms exert some stress on them. This last effect can be observed in Fig. 7, where we represent the forces that argon atoms exert on the nearby silicon in a slice taken from sample B4. The plot

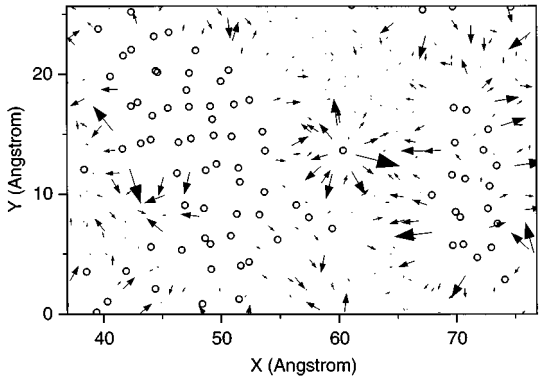

FIG. 7. Vector plot of the forces exerted by the argon atoms on the nearby silicon for a slice taken from sample B4 (8 Å thick and 5 Å below the surface). This is a front view where circles represent argon atoms and vectors silicon atoms, their magnitude being proportional to the force. As can be seen, the forces exerted by the isolated argon atom (close to the center) are stronger than in the case of the argon bubbles. Regarding to the argon bubbles, the forces are weaker for large bubbles, showing that their stability is higher.

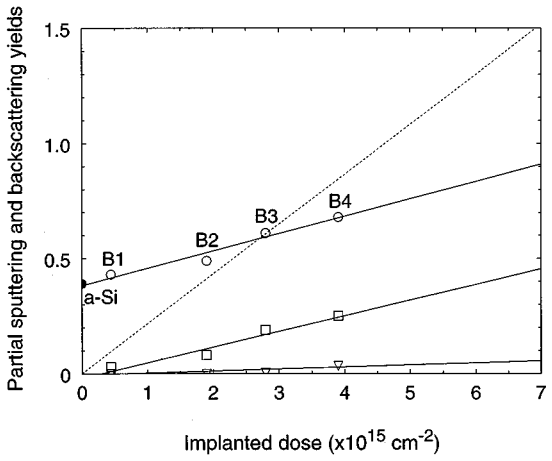

FIG. 8. Sputtering yields (circles for Si and squares for Ar) and Ar backscattering yield (triangles) obtained in the bombardment of the samples with bubbles as a function of implanted dose. The close circle represents the sputtering yield of the pure amorphous silicon sample. Solid lines are best linear fits to the data. The dashed line represents the argon yield that would be necessary to justify the steady-state silicon sputtering yield.

is a front view where circles represent argon atoms and vectors silicon atoms, their magnitude being proportional to the force. In Fig. 7, two argon bubbles and an isolated argon atom can be clearly seen. The silicon atoms are literally being pushed away by the nearby argon. It is noteworthy that the strongest forces are related to the isolated argon, while they are much weaker in the case of the bubbles. Moreover, the bigger the bubbles, the weaker the forces. Consequently, and in agreement with the experiments, it seems that the formation of relatively large argon bubbles is energetically favorable with respect to small clusters or isolated atoms for high argon concentrations.

The weakening of Si–Si bonds by the implanted argon also justifies all of the results shown in Table II. In samples with bubbles, the higher the argon concentration, the higher the silicon sputtering yield. As mentioned at the beginning of Sec. 3, the silicon yield in sample U is higher than the corresponding to sample B2, even though its argon content is lower. This is due to the uniform distribution of the argon atoms: as can be deduced from inspection of Fig. 7, when the implanted argon is uniformly distributed throughout the target the number of weakened Si–Si bonds is higher on average than when they are in bubbles. The uniform distribution of implanted argon also favors the high-yield events, as shown in Fig. 3. At the same time, when argon atoms are far from each other, their binding energies are very low, and they can escape more easily. The contrary happens when argon atoms form bubbles since they are more strongly bound.

These simulations also help understand some of the experimental observations on the evolution of the sputtering yield during argon ion bombardment. In Fig. 8, we show the relative sputtering yields for argon and silicon along with the argon backscattering yield obtained in our simulations. We present the data relative to the samples with bubbles (B1 to B4) only since this type of argon arrangement is the one readily observed in room temperature experiments, even at ion energies as low as 1 keV.[16] Taking into account the mean range of the argon ions obtained in our simulations ($\simeq$19 Å), it is possible to estimate the implanted doses that would correspond to each of our samples. As experimentally observed, the silicon sputtering yield increases linearly with dose.[2] It is noteworthy that the extrapolation to very low doses coincides quite well with the sputtering yield obtained in the bombardment of the pure amorphous silicon sample. Argon sputtering and backscattering yields also increase with dose. In all cases, the backscattering yield is very low, as observed experimentally for 1 keV argon ions with normal incidence,[19] which means that the density increase of the target does not significantly affect the percentage of backscattered argon. For every sample, and taking into account the yields obtained in our simulations, the argon incorporated during the bombardment outweighs the argon sputtering, and thus the argon content within the target increases. Since the argon sputtering yield also increases with dose, a steady state will be achieved when:

$$c = \frac{Y_{\mathrm{Ar}} - 1}{Y_{\mathrm{Si}}}, \tag{1}$$

where c represents the ratio between the number of argon and silicon atoms in the near surface region of the target. Equation (1) means that steady state conditions are reached when the ion bombardment, producing the yields Y_{Si} and Y_{Ar}, does not change the relative concentrations of the two elements near the target surface. Under those conditions, as it has also been observed experimentally, the argon content within the target saturates.[2,19] However, taking into account our results and assuming a linear behavior with dose for the Ar yield, Eq. (1) is not satisfied for any given dose, mainly due to the fact that we are not considering the argon atoms released after the collisional phase of the bombardment. Indeed, as shown in Fig. 5, argon escapes for times even longer than our total simulation time, 500 fs. This argon, coming from the subsurface bubbles, escapes due to the destabilization of the surface silicon layer and to ion-bombardment enhanced desorption. An MD simulation accounting for those effects is beyond the scope of this work, since it would be necessary to use very large samples and to follow the particle trajectories for very long times.

It has been experimentally observed that steady state conditions for 1 keV argon bombardment of silicon are reached at a dose of about 6×10^{15} cm^{-2},[15,28] which corresponds to a sample with approximately 30% argon content. From Eq. (1), to reach steady state conditions it would be necessary an argon yield of $\simeq$1.3 for that dose, which is 3.5 times higher than the value obtained from simulations up to 500 fs (dashed line in Fig. 8). However, since argon released after the collisional phase escapes with very low energies, insufficient to produce the sputtering of silicon atoms, the extension of the simulation to times longer than 500 fs would not make any difference on the measured silicon sputtering yields. This conclusion can also be inferred from Fig. 5, which shows that silicon sputtering is completed before 500 fs. In fact, for that steady state condition dose, the silicon yield predicted from our results is very close to the value

experimentally measured under steady state conditions, 0.93.[1]

IV. SUMMARY

We have carried out MD simulations on the bombardment of amorphous silicon by 1 keV argon ions in order to investigate the influence of ion accumulation on the sputtering yield. We have followed a simplified simulation scheme corresponding to different stages of the accumulation of ions in the target. The results of the simulations exhibit, and help understand, several phenomena that have been experimentally observed: desorption of shallow argon atoms, formation of solid argon bubbles, linear increase of the silicon sputtering yield with dose, enhancement of the argon sputtering yield with respect to the values expected from a pure collisional process, etc. We have observed that the increase in the silicon yield is due to the presence of shallow argon atoms that weaken Si–Si bonds, and lead to high-yield ion trajectories. On the other hand, the enhancement of the argon sputtering yield is a consequence of: (a) the low binding energies associated to implanted argon atoms (*gas sputtering*),[29] and (b) the destabilization of bubbles located very close to the surface. These two effects lead to the ejection of argon atoms even long after the end of the collision cascade. Effect (a) is important for low doses, where argon atoms are isolated or within relatively small bubbles, while effect (b) is relevant under high-dose conditions, where formation of very stable bubbles is expected.[19,28] These competing effects could lead to two different saturation regimes, as it has been observed in experiments.[28] This argon release enhancement does not seem to directly affect the silicon sputtering process, since argon atoms escape with very low energies, but it determines the dose for target saturation and thus the silicon sputtering yield value in steady state conditions. Finally, the silicon yield predicted by extrapolating our results to the saturation dose for 1 keV Ar ions is in close agreement with the experimental value.

ACKNOWLEDGMENTS

The authors are specially indebted to G. Gilmer, T. Díaz de la Rubia, and L. Colombo for useful discussions. This work was supported by the DGCYT Project No. PB92-0264 and by the Junta de Castilla y León Project No. VA40/93.

[1] P. Zalm, J. Appl. Phys. **54**, 2660 (1983).
[2] P. Blank and K. Wittmaack, J. Appl. Phys. **50**, 1519 (1979).
[3] P. Blank and K. Wittmaack, Radiat. Eff. **27**, 29 (1975).
[4] J. Kirschner and H. W. Etzkorn, Appl. Phys. A **29**, 133 (1982).
[5] K. Wittmaack, Nucl. Instrum. Methods Phys. Res. B **2**, 569 (1984).
[6] T. Okutani, M. Shikata, S. Ichimura, and R. Shimizu, J. Appl. Phys. **51**, 2884 (1980).
[7] R. A. Stansfield, K. Broomfield, and D. C. Clary, Phys. Rev. B **39**, 7680 (1989).
[8] R. Smith, D. E. Harrison, Jr., and B. Garrison, Phys. Rev. B **40**, 93 (1989).
[9] J. E. Rubio, L. A. Marqués, M. Jaraíz, L. A. Bailón, and J. Barbolla, Nucl. Instrum. Methods Phys. Res. B **102**, 301 (1995).
[10] J. M. Haile, *Molecular Dynamics Simulation, Elementary Methods* (Wiley, New York, 1992).
[11] F. H. Stillinger and T. A. Weber, Phys. Rev. B **31**, 5262 (1985).
[12] J. Tersoff, Phys. Rev. B **37**, 6991 (1988).
[13] T. Díaz de la Rubia and G. H. Gilmer, Phys. Rev. Lett. **74**, 2507 (1995).
[14] J. F. Ziegler, J. P. Biersack, and U. Littmark, *The Stopping and Range of Ions in Solids* (Pergamon, New York, 1984), Vol. 1.
[15] W. M. Lau, I. Bello, L. J. Huang, X. Feng, M. Vos, and I. V. Mitchell, J. Appl. Phys. **74**, 7101 (1993).
[16] J. C. Bean, G. E. Becker, P. M. Petroff, and T. E. Seidel, J. Appl. Phys. **48**, 907 (1977).
[17] U. Bangert, P. J. Goodhew, C. Jeynes, and I. H. Wilson, J. Phys. D **19**, 589 (1986).
[18] G. N. A. van Veen, F. H. M. Sanders, J. Dieleman, A. van Veen, D. J. Oostra, and A. E. de Vries, Phys. Rev. Lett. **57**, 739 (1986).
[19] A. van Veen, P. C. De Jong, K. R. Bijkerk, H. A. Filius, and J. H. Evans, Mater. Res. Soc. Symp. Proc. **100**, 231 (1998).
[20] G. Faraci, S. La Rosa, A. R. Pennisi, S. Mobilio, and G. Tourillon, Phys. Rev. B **43**, 9962 (1991).
[21] D. E. Harrison, Jr., N. S. Levy, L. P. Johnson III, and H. M. Effron, J. Appl. Phys. **39**, 3742 (1968).
[22] C. W. Gear, *Numerical Initial value Problems in Ordinary Differential Equations* (Prentice-Hall, Englewood Cliffs, New Jersey, 1971).
[23] L. A. Marqués, J. E. Rubio, M. Jaraíz, L. Enríquez, and J. Barbolla, Nucl. Instrum. Methods Phys. Res. B **102**, 7 (1995).
[24] P. Sigmund, in *Sputtering by Particle Bombardment I*, edited by R. Behrisch (Springer-Verlag, Heidelberg, 1981).
[25] B. J. Garrison, C. T. Reimann, N. Winograd, and D. E. Harrison, Jr., Phys. Rev. B **36**, 3516 (1987).
[26] A. Oliva, R. Kelly, and G. Falcone, Nucl. Instrum. Methods Phys. Res. B **19/20**, 101 (1987).
[27] A. A. Kosyachkov and V. T. Cherepin, Solid State Commun. **69**, 659 (1989).
[28] H. A. Filius, A. van Veen, K. R. Bijkerk, and J. H. Evans, Radiat. Eff. **108**, 1 (1989).
[29] G. Carter, D. G. Armour, S. E. Donnelly, D. C. Ingramand, and R. P. Webb, Radiat. Eff. **53**, 143 (1980).